Journal de Ciencia e Ingeniería

Journal de Ciencia e Ingeniería, Vol. 6, No. 1, Agosto de 2014, pp. 1-10
Investigación - Tecnologías Cuánticas

Underwater quantum sensing

Detección cuántica subacuática

Marco Lanzagorta [a] ⋆

[a] *US Naval Research Laboratory, 4555 Overlook Ave. SW, Washington DC 20375*

Recibido: 12/3/2014; revisado: 18/3/2014; aceptado: 10/7/2014

M. Lanzagorta: Underwater quantum sensing. Jou.Cie.Ing. **6** (1): 1-10, 2014. ISSN 2145-2628.

Abstract

In this paper we explore the possibility of underwater quantum sensing. More specifically, we analyze the performance of a quantum interferometer submerged in different types of oceanic water. Because of the strong optical attenuation produced by even the clearest ocean waters, the supersensitivity range of an underwater quantum sensor using $N = 2$ NOON entangled states is severely limited to about 18 meters, while the advantage provided by entanglement disappears at about 30 meters. As a consequence, long-range underwater quantum sensing is not feasible. Nevertheless, we discuss how underwater quantum sensing could be relevant for the detection of underwater vehicles.

***Keywords*:** Quantum information, quantum sensing, underwater sensing..

Resumen

En este articulo exploramos la posibilidad de detección cuántica subacuática. En particular, analizamos el comportamiento de un interferometro cuántico sumergido en diferentes tipos de aguas oceánicas. Debido a la fuerte atenuación óptica producida por aguas oceánicas, incluso las más puras, el rango de supersensitividad de un detector cuántico subacuático usando estados NOON con $N = 2$ está severamente limitado a una profundidad de 18 metros, mientras que la ventaja debida a los estados entrelazados desaparece a unos 30 metros. Como consecuencia, la detección cuántica subacuática de largo alcance no es posible. Sin embargo, discutimos como la detección cuántica subacuática pudiera ser importante para la detección de vehículos submarinos.

***Palabras Claves*:** Información cuántica, detectores cuánticos, detección submarina.

1. Introduction

One of the major scientific thrusts from recent years has been to try to harness quantum phenomena to dramatically increase the performance of a wide variety of classical information processing devices. In particular, it is generally accepted that quantum computers and communication systems promise to revolutionize our information infrastructure.

These advances in quantum information science have had a considerable impact on the development of quantum sensors [1]. That is, sensing devices that exploit quantum phenomena in order to increase their sensitivity. In particular, it is hoped that quantum sensors can be used to beat the standard quantum limit, which bounds the performance of most of our modern sensing

⋆ marco.lanzagorta@nrl.navy.mil

devices [2] .

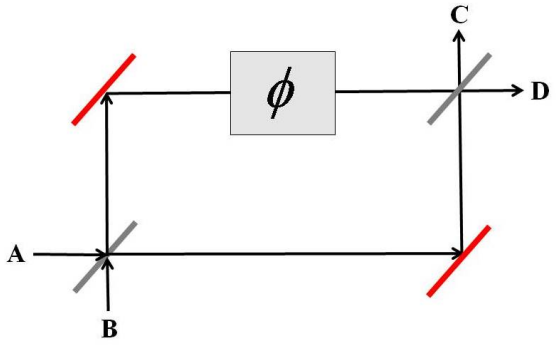

Fig. 1. Mach-Zehnder interferometer with input ports A and B, output ports C and D, and a phase delay ϕ in one of the arms.

In this paper we will consider the possibility of underwater quantum sensing. More specifically, we will analyze the performance of a Mach-Zehnder interferometer submerged in three different types of oceanic water.

To this end, let us consider the Mach-Zehnder interferometer made of two mirrors and two beam splitters as shown in Figure 2. One of the arms of the interferometer introduces an unknown phase delay ϕ. The value of ϕ can be estimated by measuring the intensity (i.e. number of photons) of the two output beams. We will consider both cases, using entangled and non-entangled photons to perform the estimation of ϕ.

2. Optical Attenuation

Any realistic description of a classical or quantum interferometer needs to account for the attenuation losses due to the medium traversed by the photons. We consider two major contributions to underwater attenuation: absorption and scattering [5]. Absorption is the process where photons are absorbed by the medium and their energy is dissipated as heat. On the other hand, scattering is the process where photons are absorbed by the medium and re-emitted in some direction with minimal thermodynamic energy dissipation. In this section we will briefly discuss attenuation in the classical and quantum realms.

2.1. *Attenuation of Classical Light*

In the context of classical electrodynamics, the energy flux of a parallel beam of light $\Phi(r)$ is attenuated due to absorption and scattering as:

$$\Phi(r) = \Phi(0)\ e^{-\chi_c r} \tag{1}$$

where χ_c is the total attenuation coefficient and can be written as:

$$\chi_c = \chi_a + \chi_b \tag{2}$$

where χ_a is the absorption attenuation coefficient and χ_b is the scattering attenuation coefficient [5].

For convenience, the oceanic waters have been divided in *Jerlov Water Types* that approximately share the same optical properties [6]. The Jerlov water types under consideration and their respective attenuation coefficients χ_c for light at $\lambda = 480$ nm are given in Table 1 [5, 6]. We have selected $\lambda = 480$ nm because this wavelength corresponds to the optical window of minimal optical attenuation in sea water [3] .

The Jerlov classification is only a matter of convenience as it may be inaccurate in many scenarios. It is important to stress that the values in Table 1 are only approximated. Indeed, the optical properties of ocean water tend to change with depth, seasonal changes, and weather effects [7]. In what follows, we will assume that the quoted value for the attenuation coefficients is constant over the range of interest.

[2] The standard quantum limit is a consequence of the discrete nature of the electromagnetic field, as well as the Poissonian statistics of classical light [2]. These properties of quantum light translate into vacuum fluctuations that affect the measurement of the amplitude of an electromagnetic field [3,4]. In a sense, these features of the quantum electromagnetic field tend to prevent the cooperative behavior of the photons [1]

[3] In general, the attenuation coefficient depends on the depth, hydrography, seasonal changes, as well as local and global atmospheric and oceanic conditions [5]

Table 1. Approximate value of the total attenuation coefficient χ_c for the three main Jerlov ocean water types for $\lambda \approx 480$ nm [5, 6].

Jerlov Type	Description	Examples	χ_c (m^{-1})
I	Clearest	Mid-Pacific and Atlantic Oceans	0.03
II	Intermediate	Northern Pacific Ocean	0.18
III	Murkiest	North Sea and East Atlantic	0.3

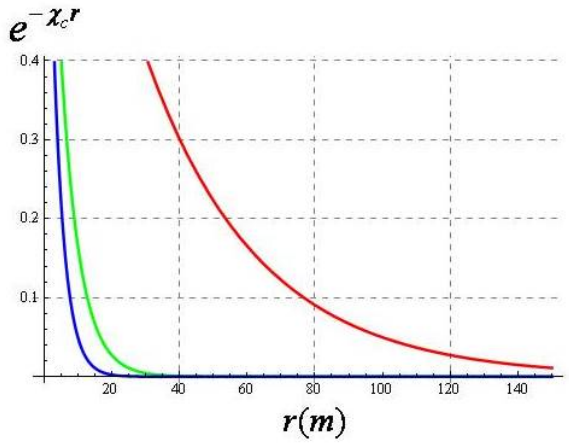

Fig. 2. Optical attenuation for $\lambda \approx 480$ nm in clear (red), intermediate (green), and murky (blue) ocean waters.

The total optical attenuation as a function of range for the underwater optical interferometer operating in three different types of oceanic waters is shown in Figure . It can be observed, for example, that for clear oceanic waters (Jerlov Type I), only 9% of the light is able to reach a depth of 80 meters, and only 5% reaches a depth of 100 meters.

2.2. *Attenuation of Quantum Light*

The quantization of the electromagnetic field in attenuating media is much more complicated than in vacuum [8–11]. For instance, the consistent theoretical treatment of attenuating media requires the quantization of interacting electromagnetic, matter, and reservoir fields [9].

While this quantization procedure is so robust that it allows the prediction of the dielectric constant of the medium, the resulting expressions are too difficult for any analytical study. Also, it is very difficult to integrate phenomenological values of the attenuation constant into the theoretical model.

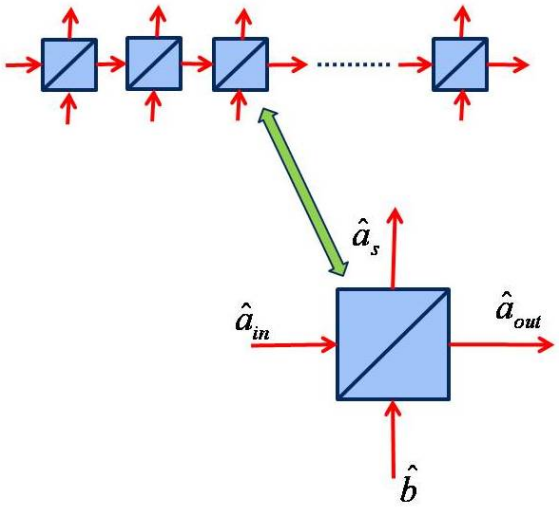

Fig. 3. The attenuation of quantum light fields (scattering + absorption) can be modeled using a chain of beam splitters [12, 13]

However, it is possible to obtain simplified equations if one assumes that the medium is adequately described by a chain of beam splitters as shown in Figure 2.2 [12,13]. The incident light field in each beam splitter is represented by the field operator $\hat{a}_{in}$. The light field that is scattered or absorbed by the medium is represented by $\hat{a}_s$. Also, the possible contributions from the medium to the light field are represented by $\hat{b}$. Finally, the net output of light is described by $\hat{a}_{out}$. Then, it can be shown that the traversal of the chain of beam splitters modifies the annihilation quantum operator into:

$$\hat{a}(\omega) \longrightarrow e^{(ik-\chi_c(\omega)/2)r}\ \hat{a}(\omega)\ +\ i\sqrt{\chi_c(\omega)}\int_0^r dx\ e^{(ik-\chi_c(\omega)/2)(r-x)}\ \hat{b}(\omega) \tag{3}$$

where:

$$k = \frac{\omega\ \eta(\omega)}{c} \tag{4}$$

and $\eta(\omega)$ is the refraction index of the medium [12, 13]. As usual, the expression for the creation operator $\hat{a}(\omega)^\dagger$ is the Hermitian-conjugate of $\hat{a}(\omega)$.

This quantization scheme offers a simpler phenomenological theory, where it is relatively easy to plug the experimental values for the attenuation coefficient χ_c. However, because of the presence of attenuation due to the external field operator $\hat{b}(\omega)$, the quantum light field has to be treated as an open quantum system [14].

As an example, let us consider the NOON state:

$$|\Psi_{NOON}\rangle = \frac{1}{\sqrt{2}}\left(|N\rangle_1|0\rangle_2 + |0\rangle_1|N\rangle_2\right) = \frac{1}{\sqrt{2}}\left(\frac{(a_1^\dagger)^N}{\sqrt{N!}} + \frac{(a_2^\dagger)^N}{\sqrt{N!}}\right)|0\rangle_1|0\rangle_2 \tag{5}$$

where the subindex identifies the arms of the interferometer [15]. After propagating each component across distances L_1 and L_2 over two different media characterized by refraction indices η_1 and η_2, and attenuation coefficients χ_{c1} and χ_{c2}, we get:

$$|\Psi'_{NOON}\rangle = \frac{1}{\sqrt{2N!}}\left[e^{-(i\omega\eta_1/c-\chi_{c1}(\omega)/2)(NL_1)}\left(\hat{a}_1^\dagger\right)^N|0\rangle_1|0\rangle_2 + e^{-(i\omega\eta_2/c-\chi_{c2}(\omega)/2)(NL_2)}\left(\hat{a}_2^\dagger\right)^N|0\rangle_1|0\rangle_2\right] + |\Phi\rangle \tag{6}$$

where $|\Phi\rangle$ is a state that represents those states that have been scattered outside the NOON basis due to the $\hat{b}(\omega)$ contribution to $\hat{a}(\omega)$.

3. Quantum Interferometry

The NOON states are often proposed for a variety of quantum sensing applications. Each half of the entangled state passes through a different arm of a Mach-Zehnder interferometer. We can assume that we are interested in measuring a phase difference ϕ that arises when photons are sent through the second arm of the interferometer [16, 17]. The effect of this phase shift ϕ on the NOON state is given by:

$$|\Psi^{(\phi)}_{NOON}\rangle = \frac{1}{\sqrt{2}}\left(|N\rangle_1|0\rangle_2 + e^{iN\phi}|0\rangle_1|N\rangle_2\right) \tag{7}$$

We can write the NOON state in terms of the creation and annihilation operators as:

$$|\Psi^{(\phi)}_{NOON}\rangle = \frac{1}{\sqrt{2}}\left(\frac{(a_1^\dagger)^N}{\sqrt{N!}}|0\rangle_1|0\rangle_2 + e^{iN\phi}\frac{(a_2^\dagger)^N}{\sqrt{N!}}|0\rangle_1|0\rangle_2\right) = \frac{1}{\sqrt{2N!}}\left((a_1^\dagger)^N + e^{iN\phi}(a_2^\dagger)^N\right)|0\rangle_1|0\rangle_2 \tag{8}$$

In order to measure the phase shift ϕ, the detector has to implement a measurement of the following observable:

$$\begin{aligned}\hat{A}_D &= |N0\rangle\langle 0N| + |0N\rangle\langle N0| \\ &= \frac{1}{N!}\left((a_1^\dagger)^N|0\rangle\langle 0|(a_2^\dagger)^N + (a_2^\dagger)^N|0\rangle\langle 0|(a_1^\dagger)^N\right)\end{aligned} \tag{9}$$

where in the sake of simplicity we have dropped the subindices labeling the arms of the interferometer.

With this setup, the amount of "noise" is given by:

$$\Delta^2 A_D = \left(\langle \hat{A}_D^2\rangle - \langle \hat{A}_D\rangle^2\right) = \sin^2 N\phi \tag{10}$$

Indeed, the noise is correlated to the phase difference ϕ introduced by the system. As expected, $\phi = 0$ implies no noise:

$$\Delta^2 A_D|_{\phi=0} = 0 \tag{11}$$

The phase responsivity is:

$$\frac{d\langle \hat{A}_D\rangle}{d\phi} = -N\sin N\phi \tag{12}$$

and the phase estimation error can be approximated by:

$$\delta\phi \approx \frac{\Delta A_D}{|\frac{d\langle \hat{A}_D\rangle}{d\phi}|} = \frac{1}{N} \tag{13}$$

That is, this interferometric phase measurement procedure using highly entangled states is able to reach the $1/N$ Heisenberg limit [16, 17].

4. Attenuated Quantum Interferometry

Let us consider the exact same interferometric experiment described above, but now the interferometer is immersed in an attenuating medium [18, 19]. The expression for the propagation of an attenuated NOON state was given in Equation (6).

In the interferometric experiment described above, the amount of noise is now given by:

$$\Delta^2 A_D = \frac{1}{2}\left(\alpha_1^N - 2\alpha_1^N\alpha_2^N + \alpha_2^N + (\alpha_1\alpha_2)^N \sin^2 N(\phi-\phi_0)\right) \tag{14}$$

while the phase responsivity is:

$$\frac{d\langle \hat{A}_D\rangle}{d\phi} = -N(\alpha_1\alpha_2)^{N/2}\sin N(\phi-\phi_0) \tag{15}$$

and we have defined the transmittance of the medium as:

$$\alpha_i \equiv e^{-\chi_{ci}L_i} \tag{16}$$

and the dispersion phase shift as:

$$\phi_0 \equiv \frac{\omega}{c}\left(\eta_2 L_2 - \eta_1 L_1\right) \tag{17}$$

Then, the phase estimation error is given by:

$$\delta\phi = \frac{\sqrt{\frac{1}{2\alpha_1^N} + \frac{1}{2\alpha_2^N} - 1 + \sin^2 N(\phi-\phi_0)}}{N\,|\sin N(\phi-\phi_0)|} \tag{18}$$

As expected, it is only in the limit of no attenuation:

$$\lim_{\alpha_1\to 1}\lim_{\alpha_2\to 1}\delta\phi = \frac{1}{N} \tag{19}$$

that the Heisenberg limit can be achieved.

5. Separable States

For comparison purposes it is useful to know the phase estimation error in the case where one uses separable states instead of entangled NOON states [18, 19]. The state (without attenuation) is taken to be:

$$|\Psi_S\rangle = \frac{1}{\sqrt{2^N}}\left(|10\rangle + |01\rangle\right)^{\otimes N} \tag{20}$$

which can be rewritten as:

$$|\Psi_S\rangle = \frac{1}{\sqrt{2^N}}\prod_{j=1}^{N}\left(\hat{a}_1^{\dagger(j)} + \hat{a}_2^{\dagger(j)}\right)|0\rangle_1|0\rangle_2 \tag{21}$$

The observable for separable states is:

$$\hat{A}_S = \bigoplus_{j=1}^{N}\left(|01\rangle^{(j)(j)}\langle 10| + |10\rangle^{(j)(j)}\langle 01|\right) \tag{22}$$

Introducing the attenuation of the states as we did before, we obtain the following variance on the phase measurement:

$$\Delta^2 A_S = \frac{N}{2}\left(\alpha_1 - 2\alpha_1\alpha_2 + \alpha_2\right) + N\,\alpha_1\alpha_2\,\sin^2(\phi-\phi_0) \tag{23}$$

and a phase responsivity:

$$\frac{d\langle \hat{A}_S\rangle}{d\phi} = -N\sqrt{\alpha_1\alpha_2}\,\sin(\phi-\phi_0) \tag{24}$$

As a consequence, the phase estimation error is:

$$\delta\phi = \frac{\sqrt{\frac{1}{2\alpha_1} + \frac{1}{2\alpha_2} - 1 + \sin^2(\phi-\phi_0)}}{\sqrt{N}\,|\sin(\phi-\phi_0)|} \tag{25}$$

which in the no-absorption limit takes the value:

$$\lim_{\alpha_1\to 1}\lim_{\alpha_2\to 1}\delta\phi = \frac{1}{\sqrt{N}} \tag{26}$$

As expected, separable states cannot be used to beat the $1/\sqrt{N}$ standard quantum limit even in the absence of attenuation.

6. Underwater Quantum Interferometry

Let us analyze a quantum interferometer submerged in Jerlov oceanic water type I ($\chi_c = 0.03m^{-1}$) and type II ($\chi_c = 0.18m^{-1}$) The behavior of the phase error for both cases can be observed in Figure 6 using $N = 2$ entangled NOON states for distances of 10 and 30 meters (type I) and 2 and 4 meters (type II). The phase estimation error depends on the value of ϕ and it never reaches the Heisenberg limit (the vertical line at $\delta\phi = 0.5$). As one would expect, the phase estimation error increases as the attenuation coefficient increases. Furthermore, the phase estimation error increases with the range to the target.

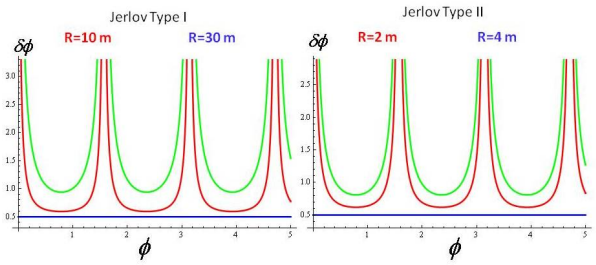

Fig. 4. Phase estimation error for Jerlov oceanic water type I ($\chi_c = 0.03m^{-1}$) and II ($\chi_c = 0.18m^{-1}$).

Let us now consider a quantum interferometer submerged in Jerlov oceanic water type I ($\chi_c = 0.03m^{-1}$) and in a hypothetical oceanic water with an attenuation twice as large ($\chi_c = 0.06m^{-1}$). The range to target is fixed at 15 meters. The behavior of the phase estimation error is shown in Figure 6. Once again, the phase estimation error increases as the attenuation coefficient increases. It can be observed that the effect of this change on the minimum phase estimation error is substantial.

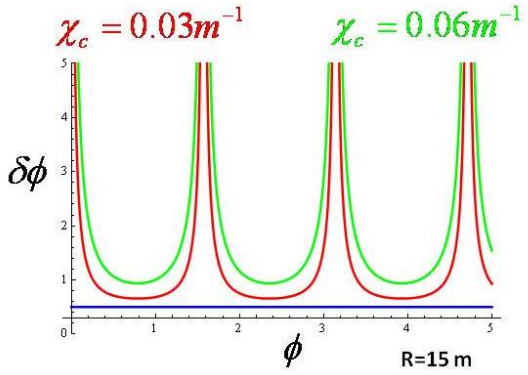

Fig. 5. Phase estimation error for Jerlov oceanic water type I ($\chi_c = 0.03m^{-1}$) and a hypothetical oceanic water with an attenuation twice as large ($\chi_c = 0.06m^{-1}$).

But perhaps more dramatic, it can be observed that the phase estimation error diverges when the sine function in the denominator of Equation (18). is close to zero. The number of divergent points in a range of values of ϕ depends on the number of photons N. Figure 6 compares the case of 2, 4, and 8 photons. The reason for these divergences is not physical, but a consequence of the approximation used for the phase estimation error:

$$\delta\phi \approx \frac{\Delta A_D}{|\frac{d\langle \hat{A}_D \rangle}{d\phi}|} = \frac{\sqrt{\frac{1}{2\alpha_1^N} + \frac{1}{2\alpha_2^N} - 1 + \sin^2 N(\phi - \phi_0)}}{N\,|\sin N(\phi - \phi_0)|} \tag{27}$$

which does not hold well in the regions where the sine function in the denominator becomes zero. That is, the approximation does not hold for those points near:

$$N\,(\phi - \phi_0) \approx 0, \pi, 2\pi, ..., n\pi \tag{28}$$

where n is an integer number.

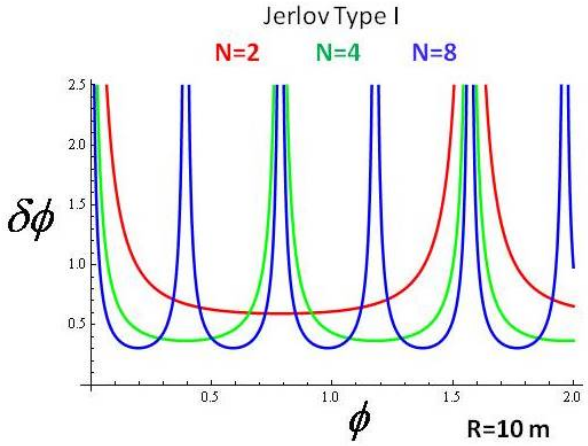

Fig. 6. Phase estimation error for 2, 4 and 10 entangled photons. The higher the number of photons, the more divergence points are found.

In any event, one can see that the phase estimation error is minimal when the sine function in the denominator is 1. That is:

$$\delta\phi_{min}^{(e)} \approx \frac{1}{N}\sqrt{\frac{1}{2\alpha_1^N} + \frac{1}{2}} \tag{29}$$

where we have ignored the contribution from the second arm, assuming it is in a well controlled, non-attenuating, environment inside the sensing apparatus.

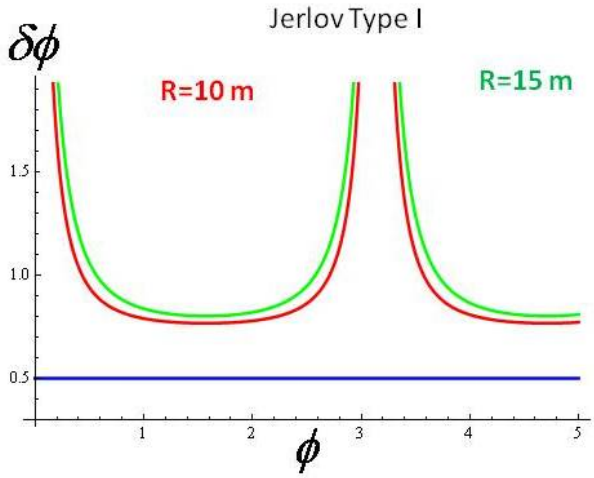

Fig. 7. Phase estimation error using $N = 2$ non-entangled photons.

As shown in Figure 6, a similar behavior is observed in the case of quantum interferometry using separable states. In this case, however, the minimum value of the phase estimation error is given by:

$$\delta\phi_{min}^{(ne)} \approx \frac{1}{\sqrt{N}}\sqrt{\frac{1}{2\alpha_1} + \frac{1}{2}} \tag{30}$$

Notice that in the limit of no attenuation, Equations (29) and (30) reduce to the Heisenberg limit and to the standard quantum limit, respectively.

Now let us assume that somehow we reach the minimum phase estimation error. The range of the detection system for the entangled (Ψ_e) and non-entangled (Ψ_{ne}) cases are shown in Figure 6. As expected, the entangled system is able to reach the Heisenberg limit (HL) at very small distances, while the separable state merely reaches the standard quantum limit (SQL). For an attenuation corresponding to Jerlov oceanic water type I, the estimation process using entangled states exceeds

the standard quantum limit up to about 18 meters. On the other hand, as shown in Figure 6, this supersensitivity is restricted to about 3 and 2 meters in the case of Jerlov oceanic water type II and III, respectively. Clearly, the extent of the supersensitivity regime, where $HL \leq \delta\phi \leq SQL$, depends on the seawater attenuation coefficient.

As a consequence, these observations make evident that supersensitive long-range underwater phase estimation using basic quantum interferometry with NOON states is severely restricted due to the attenuating effects of ocean water. However, this only means that NOON states alone are not enough to build a robust long-range supersensitive interferometric quantum sensor for practical applications.

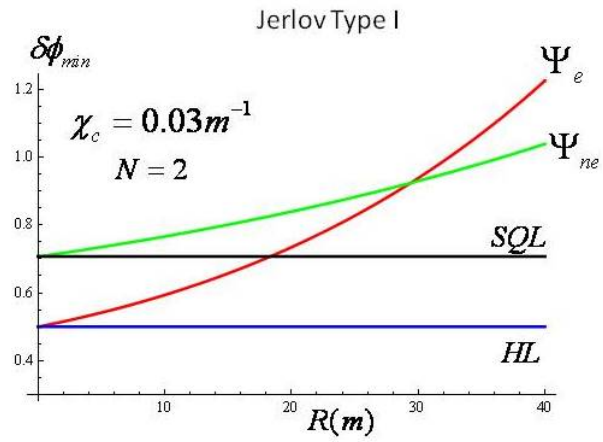

Fig. 8. Minimum phase estimation error as a function of the range to the target for $N = 2$ entangled Ψ_e and non-entangled Ψ_{ne} photons in Jerlov oceanic water type I.

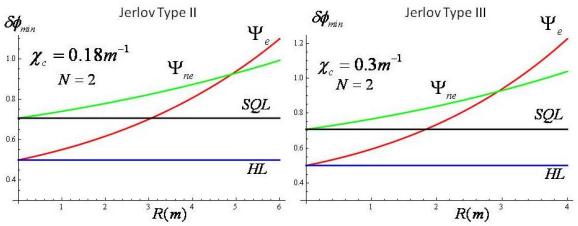

Fig. 9. Minimum phase estimation error as a function of the range to the target for $N = 2$ entangled Ψ_e and non-entangled Ψ_{ne} photons in Jerlov oceanic water type II and III.

It is also important to observe that, for long distances the sensitivity of the entangled system becomes worse than for the non-entangled system. This is observed to happen at about 30 meters in Figure 6 for the scenario corresponding to Jerlov oceanic water type I. Similar effects are observed in Figure 6, at about 5 meters for the type II scenario and at about 3 meters for type III waters. That is, for the high visibility case, the use of entanglement brings an improvement in phase measurement up to about 30 meters.

In Figures 6 and 6 we can observe the performance of the system when we use a larger number of entangled states in the NOON state. The case for $N = 10$ is shown. It can be observed that in the case of Jerlov oceanic water type I, supersensitivity is achieved up to about 9 m, and at about 1 m for type III.

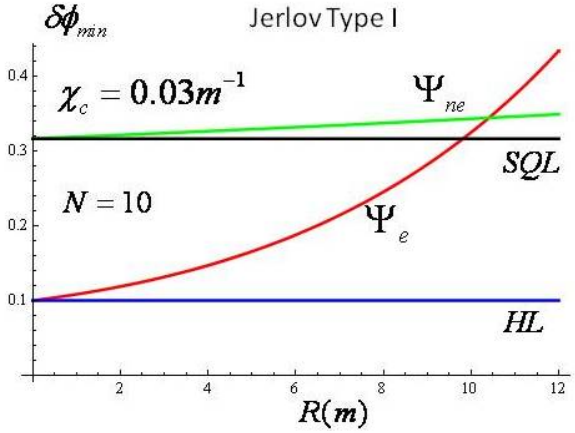

Fig. 10. Phase estimation error as a function of the range to the target for $N = 10$ entangled Ψ_e and non-entangled Ψ_{ne} photons in Jerlov oceanic water type I.

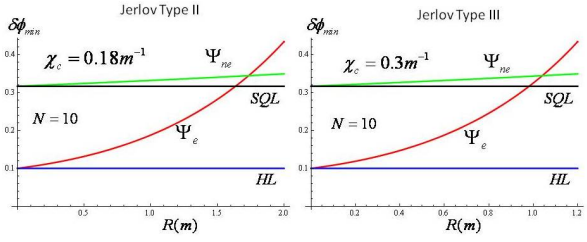

Fig. 11. Phase estimation error as a function of the range to the target for $N = 10$ entangled Ψ_e and non-entangled Ψ_{ne} photons in Jerlov oceanic water type II and III.

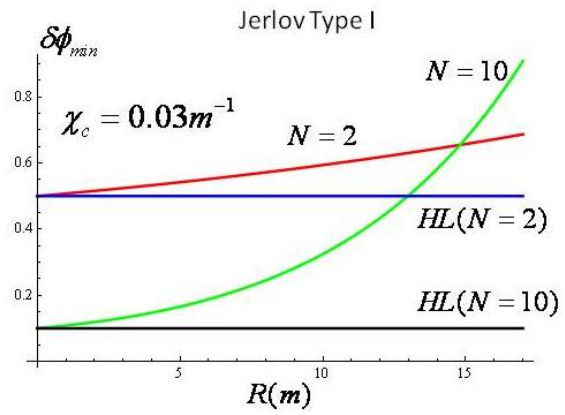

Fig. 12. Phase estimation error for N = 2 and N = 10 for Jerlov Type I ocean waters.

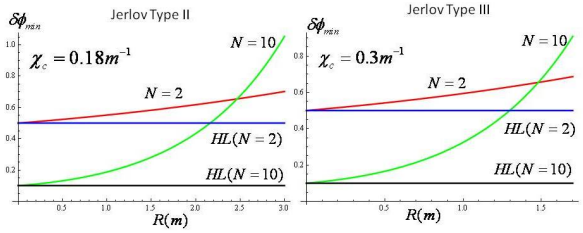

Fig. 13. Phase estimation error for N = 2 and N = 10 for Jerlov Type II and III ocean waters.

Figures 6 and 6 compare the minimum phase estimation error for $N = 2$ and $N = 10$. As expected, at short distances the minimum phase estimation error is reduced as N increases. However, the performance of the highly entangled states degrades more quickly than for the simpler entangled state.

Finally, it is worth comparing the performance of quantum interferometry in air and water. In Figure 6 we show the phase estimation error for an attenuation coefficient of 0.87 dB/km ($\chi_c \approx 0.0002m^{-1}$) which corresponds to $\lambda = 480$ nm light traversing average atmospheric conditions. It can be observed that range of super-sensitivity is of about 2,800 meters.

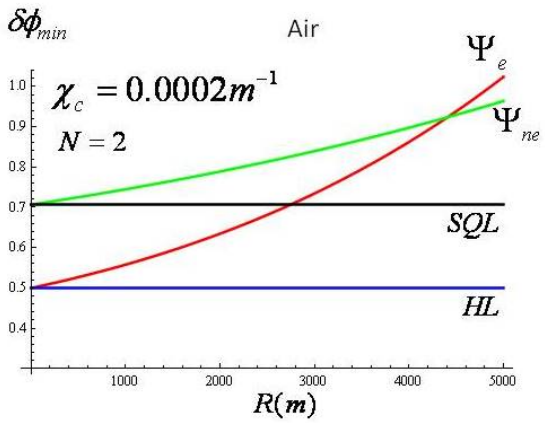

Fig. 14. Atmospheric attenuation for the phase estimation error.

All the effects so far described are a consequence of ocean water attenuation. If a quantum interferometer system operates in a perfect vacuum for which $\chi_c = 0$, then the sensor using NOON states would operate at its Heisenberg limit regardless of the traversed distance (and the sensor operating with non-entangled states would operate at its standard quantum limit regardless of the traversed distance).

The fact that the supersensitivity regime may reach up to 18 meters suggests that short-range phase estimation may be *feasible* using quantum interferometry with NOON states. However, many issues remain problematic. For instance, we have assumed that the detectors have perfect sensitivity. In reality this is not the case, and the imperfect performance of the sensors involved will diminish the supersensitivity regime achievable by the system.

7. Detection of Underwater Vehicles

We have seen that underwater quantum sensing is severely limited in range due to the attenuation properties of ocean water. Even in the case of the clearest ocean water (Jerlov Type I), the maximum range of a supersensitive underwater quantum sensor is of about 18 meters. And the advantage of using entangled states disappears at about 30 meters. As already stated, long-range quantum sensing is not feasible.

In spite of this negative result, there is an important area of application in which underwater quantum sensing could provide a great advantage. More specifically, underwater quantum sensing could be used to detect underwater vehicles at shallow depths (≈ 15 m).

Because of their small size, unmanned underwater vehicles exhibit radar and LIDAR stealth. In addition,

the electromagnetic fields generated by these vehicles are so small that they are very difficult to detect using magnetic anomaly detection (MAD) techniques [20]. However, a supersensitive LIDAR may be able to detect underwater vehicles traveling at a nominal depth of 15 meters. At this point it is worth to mention that most underwater operations are carried out in deep blue waters that correspond very closely to Jerlov Type I ocean waters [21].

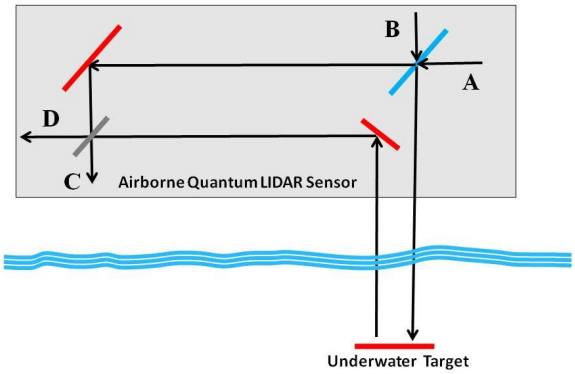

Fig. 15. Sketch of an interferometric quantum sensor used to detect a shallow underwater vehicles in naval operations.

The use of a quantum LIDAR for underwater vehicle detection in naval operations is sketched in Figure 7. The design showcases the same interferometric design discussed in the previous sections. Notice that if we ignore the attenuation due to the atmosphere and the air-water interface, then the maximum range of the underwater quantum sensor is larger than the nominal operational range of the underwater vehicle. Therefore, it is feasible that such a device could bring an advantage over the use of standard LIDAR sensing techniques in naval operations.

So far we have been talking about phase estimation, but these results can be easily generalized for the case of range-to-target estimation, the natural function of a LIDAR system. For a given wavelength λ, the range-to-target estimation error δR can be approximated by:

$$\delta R \approx \frac{\lambda}{2\pi}\delta\phi \tag{31}$$

and as a consequence, for a fixed desired spatial resolution δR:

$$\begin{aligned} \delta R^{(e)} &\geq \frac{\lambda}{2\pi\ N} \propto \frac{1}{N} \\ \delta R^{(ne)} &\geq \frac{\lambda}{2\pi\ \sqrt{N}} \propto \frac{1}{\sqrt{N}} \end{aligned} \tag{32}$$

using entangled and non-entangled states, respectively [22]. This means that for δR_{min}, the maximum resolution of the sensing device:

$$\delta R^{(e)}_{min} \propto \left(\delta R^{(ne)}_{min}\right)^2 \tag{33}$$

That is, entanglement offers a quadratic improvement in resolution over non-entangled states.

One may find surprising that if we use $\lambda = 480$ nm, then the range error in the supersensitivity regime will also be in the order of nanometers. It is not expected that a quantum LIDAR will operate at this sensitivity when detecting underwater targets. Indeed, this analysis has considered the target as a perfectly reflective and static object, which allows for a very sensitive measurement. In a sense, the scenario discussed so far resembles the situation with the Lunar Laser Ranging Experiment, which is able to measure the distance from the Earth to the Moon with milimetric accuracy [23].

8. Conclusions

In this paper we showed how, even in the case of the clearest ocean waters (Jerlov Type I), the maximum range of a supersensitive underwater quantum sensor using $N = 2$ NOON entangled states is of about 18 meters. And the advantage of using entangled states over non-entangled states disappears at about 30 meters. As a consequence, long-range underwater quantum sensing is not feasible.

Nevertheless, we argued that the detection of underwater vehicles for naval operations is a potential application of underwater quantum sensing that could bring important benefits even with its limited operational range. Still, there are several open questions that remain to be analyzed. For instance, we ignored the effect of the atmospheric column between the surface of the sea and the airborne sensor, as well as the non-trivial effects caused by the air-water interface. In addition, we did not analyzed the actual detectability of an underwater vehicle using a supersensitive quantum sensor. A more detailed study exploring these issues will be carried out in the near future.

References

[1] V. Giovannetti, S. Lloyd, and L. Maccone. Quantum-Enhanced Measurements: Beating the Standard Quantum Limit. *Science*, 306, 2004.

[2] P. Kok and B.W. Lovett. *Optical Quantum Information Processing*. Cambridge University Press, 2010.

[3] C.M. Caves. Quantum-Mechanical Noise in an Interferometer. *Phys. Rev. D*, 23(8), 1981.

[4] C.M. Caves. Quantum-Mechanical Radiation-Pressure Fluctuations in an Interferometer. *Phys. Rev. Lett.*, 45(2), 1980.

[5] K.S. Schifrin. *Physical Optics of Ocean Water*. American Institute of Physics, 1983.

[6] N.G. Jerlov. *Marine Optics*. Elsevier Science, second edition edition, 1976.

[7] J. Zanzeveld. *Variation of Optical Sea Parameters with Depth*, volume 61 of *AGARD-NATO Lecture Series*. Optics of the Sea, 1973.

[8] S.M. Dutra. *Cavity Quantum Electrodynamics*. Wiley-Interscience, 2005.

[9] B. Huttner and S.M. Barnett. Quantization of the electromagnetic field in dielectrics. *Phys. Rev. A*, 46(7), 1992.

[10] L. Knoll, S. Scheel, and D.-G. Welsch. *QED in Dispersing and Absorbing Dielectric Media*. Coherence and Statistics of Photons and Atoms. Wiley-Interscience, 2001.

[11] A. Luks and V. Perinova. *Quantum Aspects of Light Propagation*. Springer, 2009.

[12] J.R. Jeffers, N. Imoto, and R. Loudon. Quantum optics of traveling-wave attenuators and amplifiers. *Phys. Rev. A*, 47(4), 1993.

[13] R. Loudon. *The Quantum Theory of Light*. Oxford University Press, third edition edition, 2000.

[14] R. Matloob. Canonical theory of electromagnetic field quantization in dielectrics. *Optics Communications*, 192:287–297, 2001.

[15] BotoA.N. Boto, P. Kok, D. S. Abrams, S.L. Braunstein, C.P. Williams, and J.P. Dowling. Quantum interferometric optical lithography: Exploiting entanglement to beat the diffraction limit. *Phys. Rev. Lett.Lett.*, 85(13):2733–2736, 2000.

[16] L.D. Didomenico, H. Lee, P. Kok, and J.P. Dowling. Quantum Interferometric Sensors. *Proceedings of SPIE Quantum Sensing and Nanophotonic Devices*, 2004.

[17] P. Kok H. Lee and J.P. Dowling. A quantum rosetta stone for interferometry. *J. Mod. Opts.*, 49:2325, 2002.

[18] G. Gilbert, M. Hamrick, and Y. S. Weinstein. Practical Quantum Interferometry Using Photonic N00N States. In E. J. Donkor, A. R. Pirich, and H. E. Brand, editors, *Proceedings of SPIE*, Orlando, 2007.

[19] G. Gilbert and Y.S. Weinstein. Aspects of Practical Remote Quantum Sensing. *Journal of Modern Optics*, 55:3283–3291, Nov 2008.

[20] J.J. Holmes. *Exploitation of a Ship's Magnetic Field Signatures*. Morgan & Claypool, 2006.

[21] J. Hervey. Submarines. *Brassey's Sea Power, Naval Vessels, Weapons Systems and Technologies Series, Brassey's*, 4, 1994.

[22] M. Lanzagorta. *Quantum Radar*. Morgan & Claypool, 2011.

[23] *Lunar Geophysics, Geodesy, and Dynamics*. Proceedings of the 13th International Workshop on Laser Ranging, 2002.